60 Goto Y, Terajima K, Tsueshita T *et al.* Fluid resuscitation with hemoglobin-vesicle solution does not increase hypoxia or inflammatory responses in moderate hemorrhagic shock. *Biomed Res* 2006; 27: 283–8.
61 Yamazaki M, Aeba R, Yozu R, Kobayashi K. Use of hemoglobin vesicles during cardiopulmonary bypass priming prevents neurocognitive decline in rats. *Circulation* 2006; 1(Suppl.): I220–5.
62 Giarratana MC, Kobari L, Lapillonne H *et al.* Ex vivo generation of fully mature human red blood cells from hematopoietic stem cells. *Nat Biotechnol* 2005; 23: 69–74.
63 Plock JA, Contaldo C, Sakai H *et al.* Is the Hb in Hb vesicles infused for isovolemic hemodilution necessary to improve oxygenation in critically ischemic hamster skin? *Am J Physiol Heart Circ Physiol* 2005; 289: H2624–31.
64 Tsai AG, Vandegriff KD, Intaglietta M, Winslow RM. Targeted O_2 delivery by low-P_{50} hemoglobin: a new basis for O_2 therapeutics, *Am J Physiol Heart Circ Physiol* 2003; 285: H1411–9.
65 Wang L, Morizawa K, Tokuyama S, Satoh T, Tsuchida E. Modulation of oxygen-carrying capacity of artificial red cells (ARC). *Polym Adv Technol* 1992; 4: 8–11.
66 Tsai AG, Friesenecker B, McCarthy M, Sakai H, Intaglietta M. Plasma viscosity regulates capillary perfusion during extreme hemodilution in hamster skinfold model. *Am J Physiol* 1998; 275: H2170–80.
67 Sakai H, Sato A, Takeoka S, Tsuchida E. Rheological property of hemoglobin-vesicles (artificial oxygen carriers) suspended in a series of plasma substitute aqueous solutions. *Langmuir* 2007; 23: 8121–8.
68 Intaglietta M, Cabrales P, Tsai AG. Microvascular perspective of oxygen-carrying and -noncarrying blood substitutes. *Annu Rev Biomed Eng* 2006; 8: 289–321.
69 Matheson B, Kwansa HE, Bucci E, Rebel A, Koehler RC. Vascular response to infusions of a nonextravasating hemoglobin polymer. *J Appl Physiol* 2002; 93: 1479–86.
70 Contaldo C, Plock J, Sakai H *et al.* New generation of hemoglobin-based oxygen carriers evaluated for oxygenation of critically ischemic hamster flap tissue. *Crit Care Med* 2005; 33: 806–12.
71 Contaldo C, Schramm S, Wettstein R *et al.* Improved oxygenation in ischemic hamster flap tissue is correlated with increasing hemodilution with Hb vesicles and their O_2 affinity. *Am J Physiol Heart Circ Physiol* 2003; 285: H1140–7.
72 Erni D, Wettstein R, Schramm S *et al.* Normovolemic hemodilution with Hb vesicle solution attenuates hypoxia in ischemic hamster flap tissue. *Am J Physiol Heart Circ Physiol* 2003; 284: H1702–9.

Correspondence: Prof. Eishun Tsuchida, Oxygen Infusion Project, Research Institute for Science and Engineering, Waseda University, Tokyo 169-8555, Japan.
(fax: +81 3 3205 4740; e-mail: eishun@waseda.jp).

Cancer Chemother Pharmacol
DOI 10.1007/s00280-007-0636-z

ORIGINAL ARTICLE

Syndrome of inappropriate secretion of antidiuretic hormone after chemotherapy with vinorelbine

Hiroaki Kuroda · Masafumi Kawamura · Tai Hato · Kazunori Kamiya · Masahiro Kawakubo · Yotaro Izumi · Masazumi Watanabe · Hirohisa Horinouchi · Koichi Kobayashi

Received: 23 July 2007 / Accepted: 24 October 2007

Abstract
Purpose To describe a case of the syndrome of inappropriate secretion of antidiuretic hormone (SIADH) after administration of vinorelbine (VNB) for recurrence of lung cancer.
Case A 76-year-old man underwent bronchial arterial infusion (BAI) of VNB for postoperative recurrence of lung cancer. Seven days later, hyponatremia and natriuresis developed. Based on his clinical and laboratory findings, we diagnosed him with SIADH. He improved within a couple of days with fluid restriction only.
Conclusions Administration of VNB may potentially cause SIADH. This is the second report of the SIADH caused by VNB. It is important to monitor the serum sodium level and clinical findings after chemotherapy with VNB.

Keywords Syndrome of inappropriate secretion of antidiuretic hormone (SIADH) · Vinorelbine (VNB) · Non-small cell lung cancer · Chemotherapy

Introduction

We present a case of the syndrome of inappropriate secretion of antidiuretic hormone (SIADH) in a 76-year-old man after administration of vinorelbine (VNB). He underwent bronchial arterial infusion (BAI) of VNB for postoperative recurrence of lung cancer. Seven days later, hyponatremia and natriuresis developed.

Based on his clinical and laboratory findings, we diagnosed him with SIADH. He improved within a couple of days with fluid restriction only. This is the second report of the SIADH caused by VNB therapy for lung carcinoma.

H. Kuroda · M. Kawamura (✉) · T. Hato · K. Kamiya · M. Kawakubo · Y. Izumi · M. Watanabe · H. Horinouchi · K. Kobayashi
Division of General Thoracic Surgery,
School of Medicine, Keio University,
35 Shinanomachi, Shinjuku-ku, Tokyo 160-8582, Japan
e-mail: kawamura@sc.itc.keio.ac.jp

Case report

A 76-year-old man underwent left upper lobectomy for lung adenocarcinoma (pathological staging T3N1M0, stage IIIA) and 14 months later, chest computed tomography (CT) showed bilateral pulmonary metastases. Five courses of chemotherapy with docetaxel (DOC) 100 mg and gemcitabine (GEM) 1,400 mg resulted in stable disease (SD) and he was begun on modified chemotherapy with vinorelbine (VNB 40 mg). After three courses of VNB, he was admitted to hospital, complaining of left chest pain and cough.

Chest X-ray and CT on admission showed the tumor occluding in the left main bronchus and complete atelectasis of the remaining left lower lobe (Fig. 1a, b).

Transbronchial interventions, such as tumor resection, injection of ethanol and YAG laser ablation, were performed repeatedly, after which the chest X-ray showed gradual restoration in his remaining left lobe. Irradiation (total 50 Gy) of the recurrent tumor was performed for 5 weeks and then chemotherapy with VNB 40 mg (BAI 20 mg + intravenous 20 mg) was repeated.

Seven days after administration of 40 mg VNB, he complained of anorexia, nausea and lethargy. His consciousness was clear. His physical and neurogenic examinations were almost intact. His plasma sodium concentration was 113.1 mEq/l, serum osmolality was 242 mOsm/kg lower

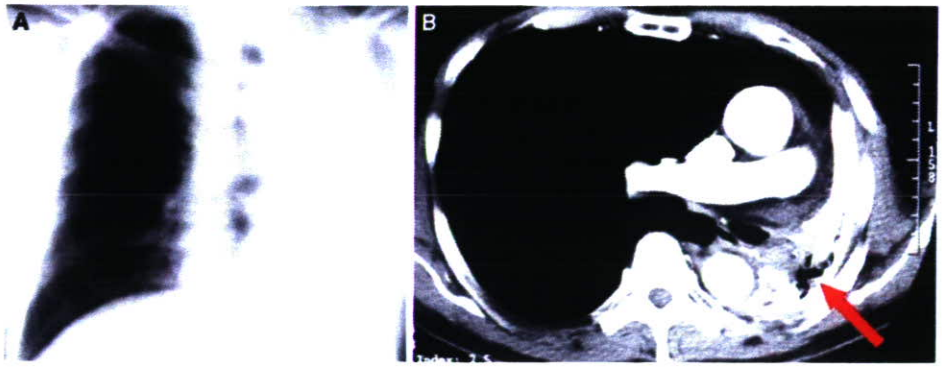

Fig. 1 **a** Chest X-ray on admission shows complete atelectasis of remaining left lobe. **b** Chest computed tomography scan shows the tumor occluding the left main bronchus (*arrow*)

than normal limit of 270 mOsm/kg and urine osmolality was 309 mOsm/kg higher than normal limit of 300 mOsm/kg. Urine sodium value was 20.2 mEq/l higher than normal limit of 20 mEq/l. His cortisol concentration value was normal. The plasma arginine vasopressin (AVP) concentration was 0.59 pg/ml, which was within normal limits, as were other parameters. Clinically, there were no symptoms related to adrenal or anterior pituitary dysfunction. The patient was euvolemic and renal function tests were within normal limits. VNB is considered to be strongly associated with SIADH, so he was diagnosed as having SIADH because his clinical features and laboratory data satisfied all standard criteria.

He was treated with water restriction, oral intake plus drip infusion into vein (DIV, total 750 ml/day). Within 2 days, his serum sodium concentration rose gradually and was restored to 130.3 mEq/l (Fig. 2). His mentation and appetite recovered in accordance with the increasing serum sodium concentration without central pontine myelinolysis. There was a possibility of developing SIADH again with a fifth cycle of VNB, so the chemotherapy agent was changed. He has been free of SIADH and has lived with lung cancer for 1 year.

Discussion

Schwartz et al. first reported SIADH in patients with lung cancer in 1957 [1]. Standard criteria include (1) hyponatremia,

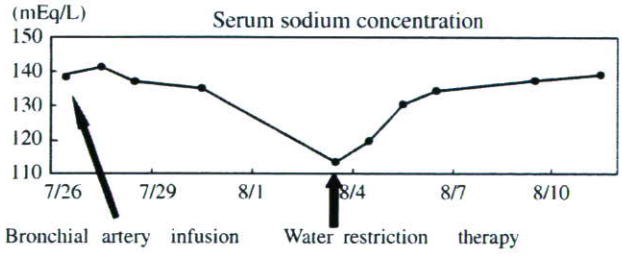

Fig. 2 Clinical course of serum sodium concentration 7 days after administration of vinorelbine. The patient complained of anorexia, nausea and lethargy and the sodium concentration was 113.1 mEq/l. He was treated with oral water restriction only and 2 days later, the serum sodium concentration was restored to 130.3 mEq/l

(2) plasma hypo-osmolality and urine hyperosmolality, (3) continuous secretion of sodium in urine, (4) normal renal function without hydration, (5) no adrenal gland dysfunction and (6) hyponatremia and hyposmotic pressure that recover with water restriction therapy without change in blood pressure [2]. The present patient fulfilled these criteria.

Various causes of SIADH have been reported, such as disorders of the cerebral nervous system, malignant tumors, diseases of the thoracic cavity, medicinal side-effects and idiopathic [3]. Approximately 75% of tumor-associated cases of SIADH are related to small-cell lung cancer (SCLC) [4]. The occurrence of SIADH with non-small-cell carcinoma (NSCLC) has been only rarely reported [5]. It has been reported that SIADH is caused by the tumor invading the vagus nerve or releasing ADH-like product. In the present study, imaging showed no evidence of invasion of the vagus nerve and we identified that the serum level of AVP was normal. We do not consider that its upregulation or secretion of ADH-like material occurred because the patient never experienced other electrolytic abnormalities and his serum sodium concentration was restored rapidly by water restriction therapy alone. There was no evidence of a relationship between progression of lung carcinoma and the onset of SIADH in this case.

Another possibility is that when the extension receptors of the left atrium detect hyperthoracic pressure and abnormal hemodynamics, they decrease the suppressor signal level and induce continuous release of ADH from the posterior lobe of the pituitary. But in the present case, bronchoscopic interventions were performed to target the local recurrence and restore his remaining left lobe. Syndrome of inappropriate secretion of antidiuretic hormone developed after 5 weeks of irradiation therapy following these interventional procedures. Even if there was a change in the respiratory circulation with release of the atelectasis, it is unlikely because of the time delay.

Enhancing release of AVP, potentiating the renal action of AVP and unknown mechanisms are reported as the main causes of SIADH by drugs [3]. Syndrome of inappropriate secretion of antidiuretic hormone associated with vinca

alkaloids, especially vincristine (VCR) and vinblastine (VBL), has been reported [6–8]. Garrett and Simpson first reported that SIADH occurred after a single treatment of VNB for breast cancer [9]. In addition, they reported that there was a slight structural difference between VNB and other vinca alkaloids, however, the precise mechanism is unclear and they may possess common neural or renal adverse effect profiles. In the present case, we firmly concluded that SIADH was induced by chemotherapy with VNB because concomitant medication was steroids only. In addition, SIADH occurred after four courses and not with earlier exposures of VNB. Although we think that repeated administration or retention of VNB may have been associated with SIADH, the precise mechanism of this SIADH was unclear.

In the report by Garrett and Simpson, SIADH from VNB did not respond to fluid restriction and patient had to be give 3% NS. But in our case, patient recovered with fluid restriction only. This difference with these two mechanisms was unclear. Furthermore, they also reported that prophylactic use of demeclocycline, which interacts with ADH at the renal collecting duct, might usefully prevent recurrence of SIADH associated with continuous treatment with VNB [9]. Stuart and Cuaso reported that SIADH was prevented by rigorous water restriction [10]. For our patients, we choose an alternative because of the high possibility of SIADH caused by VNB. If chemotherapy with VNB results in complete response or partial response, we would choose to readminister VNB with restriction of water, or use demeclocycline and monitor the sodium concentration.

We consider that VNB should be regarded as very likely to cause SIADH, but as this is only the second report of SIADH associated with use of VNB alone, it is a rare occurrence.

Conclusion

It is known that lung cancer can give rise to SIADH as a paraneoplastic syndrome and there are some anticancer agents that can potentially cause SIADH. It is important to monitor the serum sodium level and clinical findings after chemotherapy for lung cancer.

References

1. Schwartz WB, Bennet W, Curelop S, et al (1957) A syndrome of renal sodium loss and hyponatremia probably resulting from inappropriate secretion of antidiuretic hormone. Am J Med 23:529–542
2. Bartter FC, Schwartz WB (1967) The syndrome of inappropriate secretion of antidiuretic hormone. Am J Med 42:790–806
3. Reynolds RM, Seckl JR (2005) Hyponatraemia for the clinical endocrinologist. Clin Endocrinol 63:366–374
4. Tho LM, Ferry DR (2005) Is the paraneoplastic syndrome of inappropriate antidiuretic hormone secretion in lung cancer always attributable to small cell variety? Postgrad Med J 81:e17
5. Sorensen JB, Anderson, Hansen HH (1995) Syndrome of inappropriate of antidiuretic hormone (SIADH) in malignant disease. J Intern Med 238:97–110
6. Fraschini G, Recchia F, Holmes FA (1987) Syndrome of inappropriate antidiuretic hormone secretion associated with hepatic arterial infarction of vinblastine in three patients with breast cancer. Tumor 73:513–516
7. Robertson GL, Bhoopalam N, et al (1973) Vincristine neurotoxicity and abnormal secretion of antidiuretic hormone. Arch Intern Med 132:717–720
8. Kawamae K, Ganaha F, et al (1993) A case of inappropriate secretion of antidiuretic hormone (SIADH) and renal dysfunction by cisplatin. ICU CCU 17:587–592
9. Garrett CA, Simpson TA Jr (1998) Syndrome of inappropriate antidiuretic hormone associated with vinorelbine therapy. Ann Pharmacother 32:1306–1309
10. Stuart MJ, Cuaso C, et al (1975) Sydrome of recurrent increased secretion of hormone following multiple doses of vincristine. Blood 45:315–320

Journal of Surgical Research xx, xxx (2008)
doi:10.1016/j.jss.2007.12.770

Systemic Administration of Hemoglobin Vesicle Elevates Tumor Tissue Oxygen Tension and Modifies Tumor Response to Irradiation

M. Yamamoto, M.D.,* Y. Izumi, M.D., Ph.D.,*,[1] H. Horinouchi, M.D., Ph.D.,* Y. Teramura, Ph.D.,§ H. Sakai, Ph.D.,§ M. Kohno, M.D., Ph.D.,* M. Watanabe, M.D., Ph.D.,* M. Kawamura, M.D., Ph.D.,* T. Adachi, M.D., Ph.D.,† E. Ikeda, M.D., Ph.D.,‡ S. Takeoka, Ph.D.,§ E. Tsuchida, Ph.D.,§ and K. Kobayashi, M.D., Ph.D.*

*Division of General Thoracic Surgery, Department of Surgery; †Department of Biochemistry and Integrative Medical Biology; ‡Department of Pathology, School of Medicine, Keio University, Tokyo, Japan; and §Research Institute for Science and Engineering, Waseda University, Tokyo, Japan

Submitted for publication September 22, 2007

Background. **We have developed a phospholipid liposome vesicle encapsulating concentrated human hemoglobin (hemoglobin vesicle, HbV) as an artificial oxygen carrier, as an alternative to red cell transfusion. We have verified its oxygen transporting capability in a variety of preclinical models. Recent evidence suggests that artificial oxygen carriers may also be applicable for better oxygenation of ischemic or hypoxic tissues including tumors. To our knowledge, tumor oxygenation using a liposome-type artificial oxygen carrier has not been closely tested. In the present study, we tested whether systemic HbV administration changes tumor tissue oxygen tension, and if it modifies tumor response to irradiation.**

Materials and methods. **Lewis lung carcinoma was grown subcutaneously in the left hindleg of C57/BL6 mice. Experiments were initiated when the tumors reached approximately 8 mm. All experiments were done under room air. Tumor tissue oxygen tension was measured by phosphorescence quenching up to 45 min after systemic sample administration (saline: $n = 5$; HbV: $n = 5$; HbV containing methemoglobin (metHbV): $n = 4$; HbV with low oxygen affinity (lowP50HbV): $n = 8$) and compared between samples. To test the effects on irradiation response, samples (saline: $n = 7$; HbV: $n = 7$; metHbV: $n = 7$; lowP50HbV: $n = 7$) were administered prior to single 20-Gy irradiation, and tumor growth was compared.**

Results. **Tumor tissue oxygen tension transiently increased approximately 2-fold after HbV administration in comparison to other samples. Tumor growth was marginally delayed after irradiation by prior administration of HbV in comparison to other samples. HbV administration without irradiation did not affect significant tumor growth delay.**

Conclusions. **These results correlatively suggest that HbV augmented tumor growth delay following irradiation, at least in part, by affecting tumor tissue oxygen tension.**

Key Words: **hemoglobin vesicle; artificial oxygen carrier; tumor oxygenation; radiosensitizer; liposome; HIF1alpha.**

INTRODUCTION

Artificial oxygen carriers are currently being actively developed for use as transfusion alternatives. Artificial oxygen carriers do not have blood types, are free of potential infectious pathogens, and can be stored much longer than red blood cells (RBCs) [1]. Several preclinical studies indicate that they can be effectively applied as temporal resuscitative fluids, and some are undergoing clinical trials [2, 3].

Hemoglobin (Hb)-based oxygen carriers are classified into acellular chemically modified Hbs and encapsulated Hbs [4, 5]. We have developed a phospholipid liposome vesicle encapsulating concentrated human hemoglobin (hemoglobin vesicle, HbV) as an artificial oxygen carrier [1]. The cellular structure of HbV has characteristics that resemble those of RBCs. It has lipid bilayer membranes that prevent the direct contact of hemoglobin with blood components and the en-

[1] To whom correspondence and reprint requests should be addressed at Division of General Thoracic Surgery, Department of Surgery, School of Medicine Keio University, 35 Shinanomachi, Shinjuku-ku, Tokyo 160-8582, Japan. E-mail: yotaro@sc.itc.keio.ac.jp.

0022-4804/08 $34.00

dothelial lining, thus shielding the side effects of molecular hemoglobin [6, 7]. HbV particles are eventually captured by the phagocytes in the reticuloendothelial system and are metabolized through existing physiological pathways [8–10]. We have studied the oxygen transporting capabilities of HbV using several exchange transfusions, and hemorrhagic shock animal models [11–15]. In these studies, we have shown that HbV effectively restores the systemic circulation similar to red cell transfusion. Recently, evidence is accumulating that artificial oxygen carriers may be potentially applicable as so-called oxygen therapeutics, which enable oxygenation of ischemic tissues [16, 17]. Increasing tumor tissue oxygen tension is one such possibility. In the present study, we show that systemic administration of HbV transiently increases tumor tissue oxygen tension and modifies tumor response to irradiation.

MATERIALS AND METHODS

Preparation of Hemoglobin Vesicles

Preparation of poly(ethylene glycol) modified HbV was performed at Waseda University under sterile conditions as previously reported [18–20]. Hemoglobin was purified from outdated donated blood provided by Japanese Red Cross Society (Tokyo, Japan). The encapsulated hemoglobin (38 g/dL) contained 14.7 mmol/L of pyridoxal 5′-phosphate (PLP; Sigma, St. Louis, MO) as an allosteric effector at a molar ratio of Hb/PLP = 2.5. The lipid bilayer was composed of a mixture of 1,2-dipalmitoyl-*sn*-glycero-3-phosphatidylcholine, cholesterol, and 1,5-bis-*O*-hexadecyl-*N*-succinyl-L-glutamate at a molar ratio of 5/5/1 (Nippon Fine Chemicals, Osaka, Japan) and 1,2-distearoyl-*sn*-glycero-3-phosphatidylethanolamine-*N*-poly(ethylene glycol) (NOF Corp., Tokyo, Japan; 0.3 mol% of the total lipid). HbV was suspended in saline at the Hb concentration of 10 g/dL. The physicochemical parameters of the HbV were as follows: particle diameter, 251 ± 80 nm; methemoglobin concentration, <1%; HbCO concentration, <2%; and oxygen affinity (P_{50}), 29 Torr.

Preparation of Methemoglobin Vesicles

Methemoglobin vesicles (metHbV) were formed by oxidation of hemoglobin contained within HbV (methemoglobin formation), using the oxidative properties of nitrosylhemoglobin [21]. Nitric oxide gas was infused into the deoxygenated HbV suspension to transform hemoglobin to nitrosylhemoglobin. After infusion of nitrogen gas to expel the excess nitric oxide, oxygen was infused to convert nitrosylhemoglobin to methemoglobin, yielding metHbV. Vesicle properties were considered to be equivalent to HbV except for its lack of oxygen transporting ability.

Preparation of Low P50 Hemoglobin Vesicles

HbV with P_{50} of approximately 8 Torr (lowP50HbV) was prepared in the same way as HbV except that pyridoxal 5′-phosphate was not added. Particle diameter was controlled to 250 ± 64 nm. Vesicle properties were considered to be equivalent to HbV except for its P_{50}.

Animal and Tumor

Male C57/BL6 mice, approximately 9 weeks old, weighing 21 to 25 g (Oriental Yeast Co., Tokyo, Japan) were used for the experiment. The animals were housed five per cage in a specific pathogen-free, temperature-controlled, 12-h light/dark-cycled room with free access to food and water. For the experiments, the animals were anesthetized with intramuscular injection of a cocktail of 90 mg ketamine hydrochloride (Parke-Davis, Morris Plains, NJ) and 9 mg xylazine (Fermentia, Kansas City, MO) per kilogram body weight.

Lewis lung carcinoma cell line (Dainippon Sumitomo Pharma Co., Tokyo, Japan) was used for this study. In a separate group of donor mice, the tumors were grown subcutaneously and passaged. Under anesthesia, an approximately 1-mm-diameter tumor fragment was taken from the donor mouse and was placed subcutaneously in the left hindleg of mice in the experiment groups. Experiments were initiated 10 days after tumor implantation, at which time the tumors reached approximately 8 mm in diameter.

For material administration, the tail vein was cannulated under anesthesia by a 30-gauge needle and the needle was fixed by a cyanoacrylate adhesive. All experiments were carried out under room air.

All experimental protocols were reviewed by the Committee on the Ethics of Animal Experiments at School of Medicine, Keio University, and were carried out in accordance with Guidelines for Animal Experiments issued by the School of Medicine Keio University Experimental Animal Center and The Law (No. 105) and Notification (No. 6) issued by the Japanese Government. These guidelines meet the guidelines for animal handling issued by the National Institutes of Health (NIH).

Tumor Tissue Oxygen Tension Measurements

The tumor tissue oxygen tension was measured by the oxygen-dependent quenching of phosphorescence using Oxyspot phosphorimeter systems (Medical Systems Corp., Greenvale, NY). The skin over the tumor was carefully removed, and a glass coverslip was placed over the tumor. The skin on the back was also carefully removed and the back muscle was exposed followed by coverslip placement. Saline was injected under the coverslip to sustain moisture. The porphyrin probe (Oxygen Probe; Harvard Apparatus, Holliston, MA), 5,10,15,20-tetrakis(4-carboxylphenyl)porphinatoparadium, was provided as a lyophilized powder containing 9% probe, 80% bovine serum albumin (clinical grade, low fatty acid), 3% Trisma buffer, and 8% NaCl. It was dissolved in distilled water (pH 7.4) and administered through the tail vein (0.9 mL/kg). Approximately 5 min after probe administration, oxygen tension measurement was initiated. The light from the flash-lamp was filtered through an interference filter with 545-nm center wavelength and half-bandwidth of 45 nm. It was conducted through the light guide and focused on an approximately 8-mm-diameter area of the tumor tissue, approximately 4 mm from the tumor surface. The phosphorescence collected by the lens was introduced into the light guide and was filtered through a long pass filter at 645 nm, which was then led into the photomultiplier. The phosphorescence decay was fitted to a single exponential to determine the lifetime and oxygen partial pressure using the Stern–Volmer equation [22].

Measurements were made three times and averaged for each time point. Back skeletal muscle tissue oxygen tension was measured before and after tumor tissue oxygen tension measurements as control values. Tumor tissue oxygen tension was measured before (time 0), 1, 2, and 3 min after sample administration, and every 3 min thereafter until 45 min. Samples (saline: saline group, $n = 5$; HbV: HbV group, $n = 5$; metHbV: metHbV group, $n = 4$; lowP50HbV: lowP50HbV group, $n = 8$) were administered through the tail vein,12 mL/kg, in approximately 1 min.

Tumor Growth Measurements

Tumor growth measurements were made after sample administration followed by irradiation (saline: salinerad group, $n = 7$; HbV: HbVrad group, $n = 7$; metHbV: metHbVrad group, $n = 7$; lowP50HbV: lowP50HbVrad group, $n = 7$) or without irradiation (saline: salinenonrad group, $n = 5$; HbV: HbVnonrad group, $n = 4$). Single-dose irradiation (20 Gy) was delivered to the tumor-bearing

mice using a device designed for mouse bone marrow irradiation (Hitachi Medicotechnology, MBR-1520R-3, Hitachi, Japan). To irradiate only the tumor-bearing left hindlimb, a cage that shields the whole body except the tumor area from irradiation was used (Hitachi Medicotechnology, MBR-1520R-3). Power output of γ-irradiation was 150 Kv, 20 mAmp. A 0.5-mm aluminum filter was used to filtrate forward-scattered radiation. Before mouse placement, a dose measurement probe was placed inside the shield cage at the assigned tumor site, and test irradiation was done to determine the dose rate at the tumor location. Next, the probe was placed in an allocated position outside the cage, and test irradiation was done. From these two test dose rates, the dosage at the tumor site was automatically calculated in proportion to the dosage at the measurement probe. The dose rate at the tumor site was approximately 2.2 to 2.4 Gy per minute. It took approximately 8 min to complete 20-Gy irradiation using this device. Based on the measurements in tumor tissue oxygen tension following HbV administration, samples were administered approximately 10 min before the start of irradiation (salinerad, HbVrad, metHbVrad, lowP50HbVrad groups). Additionally, saline and HbV were administered without irradiation (salinenonrad, HbVnonrad groups). After sample administration with or without irradiation, the tail vein needle was removed, and the animals were allowed to recover from anesthesia. Tumors were measured using a venier caliper every 2 days up to 28 days after tumor implantation, after which point some animals started to show tumor-related distress. Estimated tumor weight was calculated as previously described [23]:

$$\text{Estimated tumor weight (mg)} = \text{longer tumor diameter (mm)} \times [\text{shorter tumor diameter (mm)}]^2/2.$$

Histological Studies and Hypoxia-Inducible Factor-1-alpha Analysis

In a separate group of animals, tumors were resected 20 min after intravenous administration of HbV ($n = 4$) or metHbV ($n = 4$). Half the tumor was fixed in 10% formalin for histology. The other half was immediately snap frozen in liquid nitrogen and stored at −80°C.

Paraffin sections were prepared from fixed tumor specimens and stained with hematoxylin and eosin for morphology. To locate HbV in tumor tissue, the human hemoglobin contained in the HbV was stained as previously described [8], with a rabbit polyclonal antibody against human hemoglobin (DAKO A/S, Copenhagen, Denmark) as the primary antibody. This antibody did not cross-react with mouse hemoglobin, which was evident from the fact that mouse RBCs were not stained. Reaction with the secondary antibody and color development were performed with the Ventana alkaline phosphatase RED detection kit using the Ventana NX system (Ventana Med. System, Inc., Tucson, AZ).

Western analysis for HIF1alpha protein was performed with the standard method. Briefly, cells were lysed with a denaturing buffer, and the lysate was centrifuged at 14,000 rpm for 15 min at 4°C. The supernatant was mixed with Laemmli buffer and applied to SDS-PAGE gels. The proteins were separated by 10% SDS-PAGE and then transferred to PVDF membrane for 90 min at 90 V using Novex Tris-Glycine system (Invitrogen, Carlsbad, CA). The primary antibody for HIF1alpha (clone 54; BD Bioscience, Franklin Lakes, NJ) was incubated with the blot overnight. The secondary anti-mouse IgG was incubated with the blots for 1 h. Bands were detected by enhanced chemiluminescence using Super Signal substrate (Pierce, Rockford, IL). Band densitometry was quantified using Image J (NIH, Bethesda, MA).

Data Analysis

Data are shown as mean ± standard deviation. Changes in tumor tissue oxygen tension and tumor growth measurements with or without irradiation were compared by analysis of variance followed by Scheffe's post-hoc test (StatView; Abacus, Berkeley, CA). Differences between groups at particular time points were compared by Mann–Whitney t-test (StatView; Abacus). Band densitometry was compared by Mann–Whitney t-test (StatView; Abacus). P values smaller than 5% were considered significant.

RESULTS

Sample administration and irradiation were well tolerated in all of the animals with no apparent changes in behavior or feeding.

Tumor Tissue Oxygen Tension Measurements

The tissue oxygen tension of back muscle before (saline: 14.4 ± 1.2; HbV: 14.2 ± 1.6; metHbV: 15.3 ± 1.2; lowP50HbV: 14.8 ± 1.2 (Torr)) and after (saline: 14.5 ± 1.1; HbV: 14.3 ± 1.4; metHbV: 15.3 ± 1.0; lowP50HbV: 14.6 ± 1.3 (Torr)) sample administration did not change significantly within or between groups. There were no significant differences in tumor tissue oxygen tension before sample administration (saline: 4.1 ± 1.1; HbV: 4.3 ± 0.8; metHbV: 4.3 ± 1.1; lowP50HbV: 4.3 ± 1.1 (Torr)). After sample administration, tumor tissue oxygen tension increased transiently in the HbV group during the observation period. Differences became significant from 15 to 30 min after sample administration in comparison to other groups. There was also a slight transient increase in the tumor tissue oxygen tension in the lowP50HbV group. Difference was significant between the saline group at 12 and 15 min after sample administration. Multiple comparisons using analysis of variance showed significant differences between HbV group curve and other groups. There was also a significant difference between lowP50HbV group curve and saline group curve (Fig. 1).

Tumor Growth Measurements

There were no significant differences in estimated tumor weight between groups at day 10 before sample administration, with or without irradiation (salinerad: 252 ± 27; HbVrad: 248 ± 38; metHbVrad: 239 ± 43; lowP50HbVrad: 248 ± 38; salinenonrad: 250 ± 33; HbVnonrad: 249 ± 38 (mg)). HbV administration without irradiation (HbVnonrad group) did not affect significant tumor growth delay in comparison to saline administration without irradiation (salinenonrad group). In both of these nonirradiated groups, tumor growth was significantly faster in comparison to any of the irradiated groups. Tumor growth delay after irradiation was marginally greater in the HbVrad group in comparison to other groups. Differences reached significance in the HbVrad group after irradiation in comparison to all other groups, from 16 to 28 days, except at day 24, at which point the difference was not significant between the metHbVrad group. Multiple comparisons

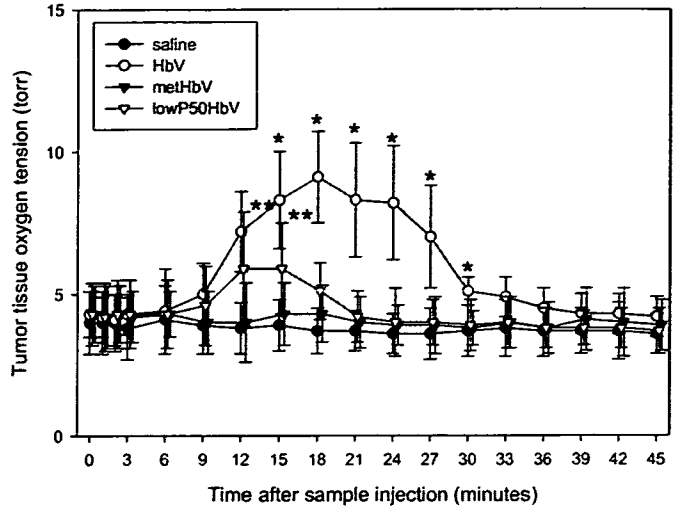

FIG. 1. Tumor tissue oxygen tension increased transiently in the HbV group. Differences became significant from 15 to 30 min after sample administration (*$P < 0.05$ *versus* all other groups, Mann–Whitney *t*-test). There was also a transient increase in the tumor tissue oxygen tension in the lowP50HbV group. Difference was significant between the saline group at 12 and 15 min after sample administration (**$P < 0.05$ *versus* saline group, Mann–Whitney *t*-test). Multiple comparisons using analysis of variance showed significant differences between the curves of HbV group and other groups. There was also a significant difference between the curves of lowP50HbV group, and saline group.

using analysis of variance showed significant differences between HbVrad group curve and all other groups (Fig. 2).

On hematoxylin and eosin staining, the tumors at day 10 were morphologically composed primarily of tumor cells, and tumor vessels, with very little extracellular matrix. Human hemoglobin staining revealed the presence of stained material not only within the tumor vessel (Fig. 3A) but also in the extracellular matrix (Fig. 3B), which were presumably extravasated HbV. On Western blot analysis, HIF1alpha level was significantly decreased in the HbV group in comparison to the metHbV group (Fig. 4).

DISCUSSION

One of the primary causes of tumor resistance to irradiation may be tumor tissue hypoxia. Although still far from conclusive in the clinic, this notion is generally accepted [24]. *In vitro* studies show that the presence of oxygen increases the cytotoxicity of irradiation, resulting in roughly a 3-fold difference in radiosensitivity between hypoxic and aerobic cells [25, 26]. This phenomenon is widely attributed to the oxygen's ability to chemically modify radiation-induced DNA damage, creating adducts that are not repaired by cells.

A correlation between tumor tissue oxygen tension status and therapeutic response after treatment with irradiation or chemotherapeutic agents has been observed in many preclinical studies. There is also accumulating clinical evidence that therapeutically significant tissue hypoxia frequently exists in human tumors. As a result, there has been a longstanding active research into novel methods of improving tumor tissue oxygenation, targeting hypoxic tumor cells, and/or modulating the effect hypoxia has on how tumors respond to treatment. Several methods of overcoming tumor tissue hypoxia are currently under investigation. These include hyperbaric oxygen, hyperthermia, and the use of potential radiosensitizers such as nitroimidazole-based substances, and pentoxifylline [27]. Artificial oxygen carriers, such as perfluorochemicals, and modified hemoglobins have also been evaluated for this purpose in several preclinical studies [28–34]. We have previously reported the effect of a totally synthetic-heme-based artificial oxygen carrier in oxygenating tumor tissue [35]. To our knowledge, tumor oxygenation using a liposome-type artificial oxygen carrier has not been closely tested.

The dose of HbV administered in this study, 12 mL/kg, is rather high in the context of a therapeutic drug. But since HbV is being developed primarily as a transfusion alternative, it should be possible to administer this dosage without complications in order for HbV to be clinically applicable. No adverse effects directly attributable to material administration were apparent with any of the administered samples. Oxygen tension of back muscle tissue did not change significantly with

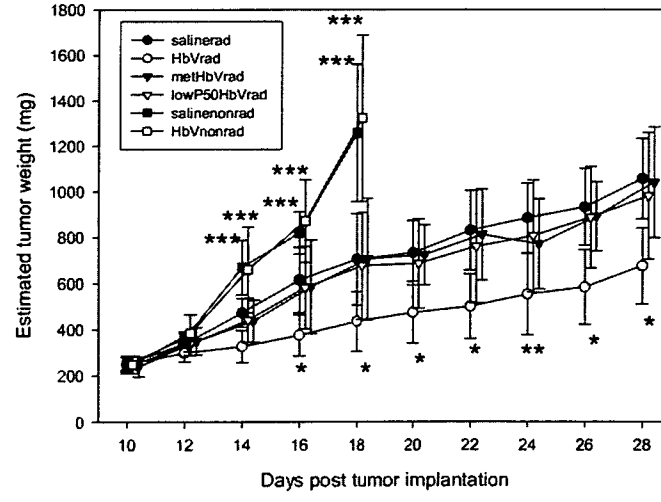

FIG. 2. Sample administration, saline, HbV, metHbV, lowP50HbV, with irradiation (salinerad, HbVrad, metHbVrad, lowP50HbVrad, groups respectively) or without irradiation (salinenonrad, HbVnonrad groups) were carried out on day 10. In the salinenonrad and HbVnonrad groups, tumor growth was significantly faster in comparison to any of the irradiated groups (***$P < 0.05$ *versus* groups that received irradiation, Mann–Whitney *t*-test). Tumor growth delay after irradiation was significantly increased in the HbVrad group in comparison to other groups (*$P < 0.05$ *versus* all other groups, Mann–Whitney *t*-test), except at day 24, at which point the difference was not significant between the metHbVrad group (**$P < 0.05$ *versus* all other groups except metHbV group, Mann–Whitney *t*-test). Multiple comparisons using analysis of variance showed a significant difference in the growth curves between HbVrad group, and all other groups.

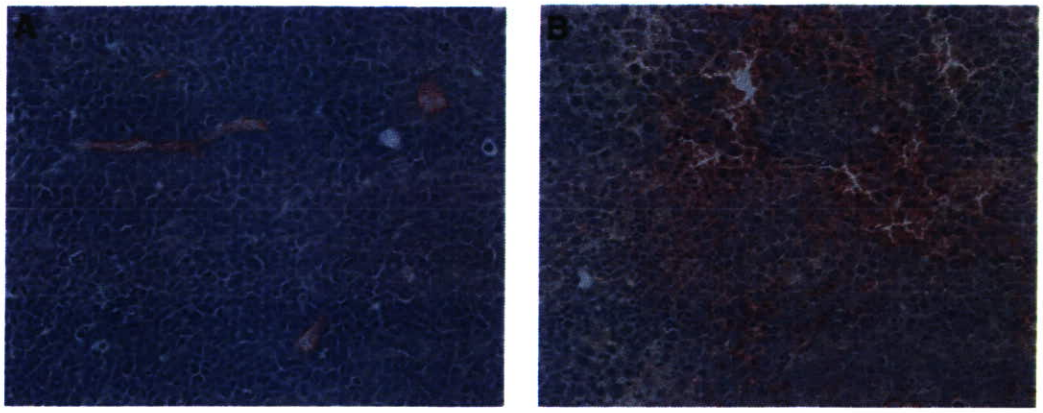

FIG. 3. Human hemoglobin staining could be seen not only within the tumor vessels (A) but also in the extracellular matrix (B) (human hemoglobin staining, ×20).

sample administration, but the measurements were made before and after the completion of tumor tissue oxygen tension measurements primarily to verify the integrity of light guide and lens. Therefore, a transient rise in muscle tissue oxygen tension as well as other normal tissues, possibly leading to toxicity, cannot be denied. Further studies are needed in this area.

In the present study, systemic administration of HbV transiently reduced tumor hypoxia, and moderately augmented tumor growth delay in response to irradiation in comparison to groups administered saline, metHbV, or lowP50HbV. HIF1alpha is a transcription factor activated by hypoxia, controlling many pathways in response to hypoxia in both normal and tumor cells. In the present study, tumor HIF1alpha protein level was significantly decreased at 20 min after HbV administration compared with metHbV administration. These results correlatively suggest that HbV augmented tumor growth delay following irradiation, at least in part, by affecting tumor tissue oxygen tension. However, the growth delay in the HbV group, although statistically significant, was marginal. A study using different irradiation dosages to determine TCD50 is necessary to further verify this effect. The involvement of other mechanisms is also possible. In the present study, metHbV administration did not have a significant effect on tumor tissue oxygen tension or irradiation response. Nevertheless, the effect of heme itself needs further investigation, because the heme within HbV could be the primary source of oxygen radical species formation following irradiation rather than the oxygen it delivers. It is also known that

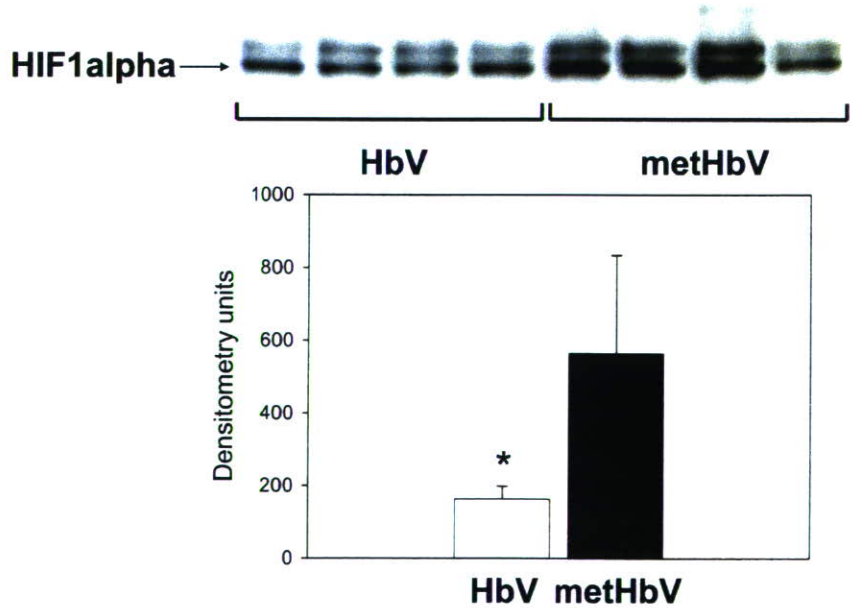

FIG. 4. HIF1alpha level was significantly decreased in the HbV group in comparison to the metHbV group. *P = 0.021 Mann–Whitney U-Test.

changes in HIF1alpha level itself modifies irradiation response, but both radiosensitization and radioprotection by changes in HIF1alpha level have been observed [36]. Further studies, including measurements at longer time points and with administration of other samples, are required to find out if the change in HIF1alpha level, with respect to or irrespective of change in tissue oxygen tension, is involved in this particular animal model.

The timing of tumor tissue oxygen tension elevation after artificial oxygen carrier administration differs among previous reports from approximately 4 min to 2 h [9, 28–35]. We do not have a clear answer as to why the increase in tumor tissue oxygen tension was transient in the present study. If the increase in tumor tissue oxygen tension was due to circulating HbV, the effect should have appeared over a longer duration because HbV is known to have a circulating half-life of approximately 48 h [37]. Therefore, we speculated that the increase in tumor tissue oxygen tension may have been affected primarily by extravasated HbV rather than circulating HbV and was hence transient. Tumor vessels are known to be morphologically heterogeneous and has highly permeable sites in comparison to normal vessels. Liposomes ranging in diameter from approximately 100 to 400 nm have been shown to extravasate into the tumor extracellular matrix presumably through these sites [38, 39]. In the present study, human hemoglobin staining revealed the presence of stained material not only within the tumor vasculature but also in the extracellular matrix. We know from previous experiments that hemoglobin is encapsulated within HbV until it is metabolized, which does not occur in this timeframe of 20 min after systemic administration [40]. So we consider that these were extravasated HbV. Lewis lung carcinoma used in this study formed tumors composed primarily of tumor cells and tumor vessels, with very little extracellular matrix. Because of this, the extravasated HbV mostly existed in the vicinity of tumor cells, and hence, may have modulated the tumor response to irradiation. Obviously these results may not be directly applicable to tumors encountered in the clinic, which contain significantly greater amounts of extracellular matrix.

Oxyspot used in this study only measures tissue oxygen tension close to the tissue surface. But since the Lewis lung carcinoma cell line used in this study formed a histologically homogeneous tumor composed primarily from tumor cells and vessels, with little extracellular matrix, we assume that the measurements made in this study sufficiently reflected tissue oxygen tension changes within the whole tumor. To this end, Lewis lung carcinoma line was suitable for this particular study, but its clinical relevance may be limited.

It has been reported that increase in hemoglobin affinity is beneficial for oxygen delivery to normal tissue particularly when oxygen supply is severely compromised [41, 42]. In the present study, there was only a minimal transient increase in tumor tissue oxygen tension after lowP50HbV administration, and benefit was not so apparent. Physiology of oxygen extraction may have been different between different tissues or tumor lines. Blood flow in tumor vessels is known to be highly variable, and regulatory mechanisms may not have functioned as in normal tissue. P_{50} of 8 Torr in lowP50HbV used in this study may have been too low for significant oxygen release in this particular model. Additionally, in the present study, the increase in tumor tissue oxygen tension may have been due to extravasated rather than circulating HbV, in which case the findings from previous studies which examine materials with low P_{50} supplying oxygen from within the circulation may not be directly applicable. Further studies are needed to find out if optimization of P_{50} significantly contributes to oxygenating tumor tissue.

Many types of liposomes are currently being developed to improve selective drug delivery to tumor tissue. HbV used in this study was developed as a transfusion alternative, but it may be possible to increase relative tumor distribution and further optimize HbV's irradiation augmentation effect by modifying its liposomal components as well as its P_{50}. These improvements may lead to similar or better outcome, with less dosage. The timing of irradiation also needs further study, including the use of fractionation.

ACKNOWLEDGMENTS

We thank Mr. Hitoshi Abe, Department of Pathology, School of Medicine, Keio University, for expertise in immunohistochemistry.

REFERENCES

1. Kobayashi K, Tsuchida E, Horinouchi H, eds. Artificial Oxygen Carrier: Its Front Line, Keio University International Symposia for Life Sciences and Medicine. Vol. 12, Springer-Verlag, 2005.
2. Chang TM. Hemoglobin based red blood cells substitutes. Artif Organs 2004;28:789.
3. Buehler PW, Alayash AI. Toxicities of hemoglobin solutions. in search of in-vitro and in-vivo model systems. Transfusion 2004; 44:1516.
4. Djordjevich L, Mayoral J, Miller IF, et al. Cardiorespiratory effects of exchanging transfusions with synthetic erythrocytes in rats. Crit Care Med 1987;15:318.
5. Awasthi VD, Garcia D, Klipper R, et al. Neutral and anionic liposome-encapsulated hemoglobin: effect of postinserted poly-(ethylene glycol)-distearoylphosphatidylethanolamine on distribution and circulation kinetics. J Pharmacol Exp Ther 2004; 309:241.
6. D'Agnillo F, Alayash AI. Redox cycling of diaspirin cross-linked hemoglobin induces G2/M arrest and apoptosis in cultured endothelial cells. Blood 2001;98:3315.
7. Sakai H, Hara H, Yuasa M, et al. Molecular dimensions of Hb-based O(2) carriers determine constriction of resistance arteries and hypertension. Am J Physiol Heart Circ Physiol 2000; 279:H908.

8. Sakai H, Horinouchi H, Yamamoto M, et al. Acute 40 percent exchange-transfusion with hemoglobin-vesicles (HbV) suspended in recombinant human serum albumin solution: Degradation of HbV and erythropoiesis in a rat spleen for 2 weeks. Transfusion 2006;46:339.
9. Sakai H, Horinouchi H, Tomiyama K, et al. Hemoglobin-vesicles as oxygen carriers: Influence on phagocytic activity and histopathological changes in reticuloendothelial system. Am J Pathol 2001;159:1079.
10. Sakai H, Masada Y, Horinouchi H, et al. Physiological capacity of the reticuloendothelial system for the degradation of hemoglobin vesicles (artificial oxygen carriers) after massive intravenous doses by daily repeated infusions for 14 days. J Pharmacol Exp Ther 2004;311:874.
11. Izumi Y, Sakai H, Hamada K, et al. Physiologic responses to exchange transfusion with hemoglobin vesicles as an artificial oxygen carrier in anesthetized rats: Changes in mean arterial pressure and renal cortical tissue oxygen tension. Crit Care Med 1996;24:1869.
12. Izumi Y, Sakai H, Kose T, et al. Evaluation of the capabilities of a hemoglobin vesicle as an artificial oxygen carrier in a rat exchange transfusion model. ASAIO J 1997;43:289.
13. Sakai H, Takeoka S, Wettstein R, et al. Systemic and microvascular responses to the hemorrhagic shock and resuscitation with Hb-vesicles. Am J Physiol Heart Circ Physiol 2002;283: H1191.
14. Sakai H, Masada Y, Horinouchi H, et al. Hemoglobin-vesicles suspended in recombinant human serum albumin for resuscitation from hemorrhagic shock in anesthetized rats. Crit Care Med 2004;32:539.
15. Yoshizu A, Izumi Y, Park S, et al. Hemorrhagic shock resuscitation with an artificial oxygen carrier, hemoglobin vesicle, maintains intestinal perfusion and suppresses the increase in plasma tumor necrosis factor-alpha. ASAIO J 2004;50:458.
16. Contaldo C, Plock J, Sakai H, et al. New generation of hemoglobin-based oxygen carriers evaluated for oxygenation of critically ischemic hamster flap tissue. Crit Care Med 2005;33:806.
17. Nozue M, Lee I, Manning JM, et al. Oxygenation in tumors by modified hemoglobins. J Surg Oncol 1996;62:109.
18. Takeoka S, Ohgushi T, Terase K, et al. Layer-controlled hemoglobin vesicles by interaction of hemoglobin with a phospholipid assembly. Langmuir 1996;12:1755.
19. Sakai H, Takeoka S, Park SI, et al. Surface-modification of hemoglobin vesicles with polyethyleneglycol and effects on aggregation, viscosity, and blood flow during 90%-exchange transfusion in anesthetized rats. Bioconjug Chem 1997;8:15.
20. Sakai H, Yusua M, Onuma H, et al. Synthesis and physicochemical characterization of a series of hemoglobin-based oxygen carriers: Objective comparison between cellular and acelluar types. Bioconjug Chem 2000;11:56.
21. Maeda N, Imaizumi K, Kon K, et al. A kinetic study on functional impairment of nitric oxide-exposed rat erythrocytes. Environ Health Perspect 1987;73:171.
22. Wilson DF, Cerniglia GJ. Localization of tumors and evaluation of their state of oxygenation by phosphorescence imaging. Cancer Res 1992;52:3988.
23. Ishikawa Y, Kubota T, Otani Y, et al. Dihydropyrimidine dehydrogenase activity and messenger RNA level may be related to the antitumor effect of 5-fluorouracil on human tumor xenografts in nude mice. Clin Cancer Res 1999;5:883.
24. Moeller BJ, Richardson RA, Dewhirst MW. Hypoxia and radiotherapy: Opportunities for improved outcomes in cancer treatment. Cancer Metastasis Rev 2007;26:241.
25. Gray LH, Conger AD, Ebert M, et al. The concentration of oxygen dissolved in tissues at the time of irradiation as a factor in radiotherapy. Br J Radiol 1953;26:638.
26. Deschner EE, Gray LH. Influence of oxygen tension on x-ray-induced chromosomal damage in Ehrlich ascites tumor cells irradiated in vitro and in vivo. Radiat Res 1959;11:115.
27. Lee I, Kim JH, Levitt SH, et al. Increases in tumor response by pentoxifylline alone or in combination with nicotinamide. Int J Radiat Oncol Biol Phys 1992;22:425.
28. Teicher BA, Herman TS, Hopkins RE, et al. Effect of oxygen level on the enhancement of tumor response to radiation by perfluorochemical emulsions or a bovine hemoglobin preparation. Int J Radiat Oncol Biol Phys 1991;21:969.
29. Teicher BA, Holden SA, Ara G, et al. Effect of a bovine hemoglobin preparation (SBHS) on the response of two murine solid tumors to radiation therapy or chemotherapeutic alkylating agents. Biomater Artif Cells Immob Biotechnol 1992;20:657.
30. Teicher BA, Herman TS, Menon K. Enhancement of fractionated radiation therapy by an experimental concentrated perflubron emulsion (Oxygent) in the Lewis lung carcinoma. Biomater Artif Cells Immob Biotechnol 1992;20:899.
31. Teicher BA, Dupuis NP, Robinson MF, et al. Reduced oxygenation in a rat mammary carcinoma post-radiation and reoxygenation with a perflubron emulsion/carbogen breathing. In Vivo 1994;8:125.
32. Teicher BA. An overview on oxygen carriers in cancer therapy. Artif Cells Blood Substit Immobil Biotechnol 1995;23:395.
33. Robinson MF, Dupuis NP, Kusumoto T, et al. Increased tumor oxygenation and radiation sensitivity in two rat tumors by a hemoglobin-based, oxygen-carrying preparation. Artif Cells Blood Substit Immobil Biotechnol 1995;23:431.
34. Linberg R, Conover CD, Shum KL, et al. Increased tissue oxygenation and enhanced radiation sensitivity of solid tumors in rodents following polyethylene glycol conjugated bovine hemoglobin administration. In Vivo 1998;12:167.
35. Kobayashi K, Komatsu T, Iwamaru A, et al. Oxygenation of hypoxic region in solid tumor by administration of human serum albumin incorporating synthetic hemes. J. Biomed Mater Res A 2003;64:48.
36. Moeller BJ, Dewhirst MW. HIF-1 and tumour radiosensitivity. Br J Cancer 2006;95:1.
37. Sou K, Klipper R, Goins B, et al. Circulation kinetics and organ distribution of Hb-vesicles developed as a red blood cell substitute. J Pharmacol Exp Ther 2005;312:702.
38. Yuan F, Dellian M, Fukumura D, et al. Vascular permeability in a human tumor xenograft: Molecular size dependence and cutoff size. Cancer Res 1995;55:3752.
39. Yuan F, Leunig M, Huang SK, et al. Microvascular permeability and interstitial penetration of sterically stabilized (stealth) liposomes in a human tumor xenograft. Cancer Res 1994;54: 3352.
40. Takeoka S, Teramura Y, Atoji T, et al. Effect of Hb-encapsulation with vesicles on H_2O_2 reaction and lipid peroxidation. Bioconjug Chem 2002;13:1302.
41. Stein JC, Ellsworth ML. Capillary oxygen transport during severe hypoxia: Role of hemoglobin oxygen affinity. J Appl Physiol 1993;75:1601.
42. Sakai H, Cabrales P, Tsai AG, et al. Oxygen release from low and normal P_{50} Hb vesicles in transiently occluded arterioles of the hamster window model. Am J Physiol Heart Circ Physiol 2005;288:H2897.

PII: S1570-9639(08)00096-4
DOI: doi: 10.1016/j.bbapap.2008.03.007
Reference: BBAPAP 37903

To appear in: *BBA - Proteins and Proteomics*

Received date: 27 November 2007
Revised date: 16 February 2008
Accepted date: 10 March 2008

Please cite this article as: Hiromi Sakai, Atsushi Sato, Peter Sobolewski, Shinji Takeoka, John A. Frangos, Koichi Kobayashi, Marcos Intaglietta, Eishun Tsuchida, NO and CO binding profiles of hemoglobin vesicles as artificial oxygen carriers, *BBA - Proteins and Proteomics* (2008), doi: 10.1016/j.bbapap.2008.03.007

NO and CO Binding Profiles of Hemoglobin Vesicles as Artificial Oxygen Carriers

Hiromi Sakai[a], Atsushi Sato[b], Peter Sobolewski[c,d], Shinji Takeoka[b], John A. Frangos[c], Koichi Kobayashi[e], Marcos Intaglietta[c,d], and Eishun Tsuchida[a]*

[a] *Research Institute for Science and Engineering, Waseda University, Tokyo 169-8555, Japan;*
[b] *Graduate School of Science and Engineering, Waseda University, Tokyo 169-8555, Japan;*
[c] *La Jolla Bioengineering Institute, La Jolla, CA, 92037, USA;*
[d] *Department of Bioengineering, University of California, San Diego, La Jolla, CA, 92093-0412, USA*
[e] *Department of Surgery, School of Medicine, Keio University, Tokyo 160-8582, Japan*

Key Words: Blood substitutes / Artificial red cells / Liposome / NO / CO / Vasoconstriction

Running title: Hb-vesicle as an O_2-carrier

.....

* To whom correspondence should be addressed.
Eishun Tsuchida, Professor
Research Institute for Science and Engineering, Waseda University, Tokyo 169-8555, Japan.
Phone +81-3-5286-3120; Fax +81-3-3205-4740; e-mail eishun@waseda.jp

Abbreviations: HbV, hemoglobin-vesicles; RBC, red blood cells; $k'_{on}{}^{(NO)}$, apparent NO binding rate constant; $k'_{on}{}^{(CO)}$, apparent CO binding rate constant; apparent CO binding rate constant; $k'_{OX}{}^{(NO)}$, apparent oxidation rate by NO; PLP, pyridoxal 5'-phosphate; DPPC, 1,2-dipalmitoyl-*sn*-glycero-3-phosphatidylcholine

Summary

Hemoglobin vesicles (HbVs) are artificial oxygen carriers encapsulating purified and concentrated Hb solution in phospholipid vesicles (liposomes). We examined in-vitro reaction profiles of a formulation of HbV with NO and CO in anaerobic and aerobic conditions using stopped-flow spectrophotometry and a NO electrode. Reaction rate constants of NO to deoxygenated and oxygenated HbV were considerably smaller than those of cell free-Hb because of the intracellular NO-diffusion barrier. The reaction of CO with deoxygenated HbV was slightly slower than that of cell free-Hb solely because of the co-encapsulated allosteric effector, pyridoxal 5'-phosphate. The NO depletion in an aerobic condition in the presence of empty vesicles was monitored using a NO electrode, showing that the hydrophobic bilayer membrane of HbV, which might have higher gas solubility, does not markedly facilitate the O_2 and NO reaction, and that the intracellular Hb is the major component of NO depletion. In conclusion, HbV shows retarded gas reactions, providing some useful information to explain the absence of vasoconstriction and hypertension when they are intravenously injected.

1. Introduction

A physiologically important aspect of the structure of red blood cells (RBCs) is the management of the transport of endogenous gaseous messenger molecules (NO and CO) [1-3]. Conditions of hemolysis [4] and studies related to the development of hemoglobin-based oxygen carriers (HBOCs) [5-11] have shown that the entrapment of endothelium-derived NO induces vasoconstriction, hypertension, reduced blood flow, and vascular damage. Physiological doses of CO are a vasorelaxation factor, especially in the hepatic microcirculation [12] and its entrapment by cell-free hemoglobin (Hb) solutions induces constriction of sinusoidal capillaries [13]. These side effects due to the presence of molecular Hb in plasma suggest that the cellular structure of RBCs plays a role in insuring the bioavailability of NO and CO.

Several mechanism have been proposed to explain NO binding retardation by Hb encapsulation in RBCs [14-16], namely: (i) an unstirred layer forming an extracellular diffusion barrier surrounding the RBC [2,14]; (ii) a protein-rich RBC cytoskeletal submembrane constituting a physical barrier against NO diffusion [17,18]; and (iii) retardation of gas diffusion due to the viscosity of the Hb solution in RBCs [19].

Hemoglobin has been encapsulated using lipid bilayer membranes to form of Hb vesicles (HbV), in order to produce a blood like HBOC where the oxygen carrying Hb is not dissolved in plasma [20,21]. In this configuration Hb is not vasoactive [9,10], an effect in part due to the retardation of NO binding by Hb encapsulation in phospholipid vesicles [22]. Furthermore, using results of stopped-flow spectrophotometry and computer simulation, we recently determined that the major component of retardation is the intracellular rather than the extracellular diffusion barrier. This conclusion is also supported by considering that: (i) the

large binding rate constant of NO to a heme in an Hb molecule, (ii) the numerous hemes as sites of gas entrapment at a high intracellular Hb concentration $[Hb]_{in}$, (iii) the slowed gas diffusion in the intracellular viscous Hb solution; and (iv) the lipid bilayer membrane of HbV would not possess any barrier function to the NO diffusion into the particles [23].

On the other hand, the hydrophobic part of a cell membrane reportedly possesses higher gas solubility than the bulk aqueous phase. Both NO and O_2 dissolve to a greater extent in the hydrophobic part, which facilitates the reaction of NO with O_2 to produce NO_2^- [24]. HbV mimics the structure of RBCs, however the particle diameter is much smaller than that of RBCs, and the surface to volume ratio is larger. Therefore for the same oxygen carrying capacity, or equivalent cell concentration by volume there is proportionally greater amount of membrane material for HbVs than for RBCs providing a greater hydrophobic domain. This structural difference is important because it is likely that there is NO depletion in the lipid bilayer membrane of HbVs.

In the present study we analyzed the NO and CO binding rates of HbV with the present formulation, along with the possibility of accelerated NO depletion in the hydrophobic domain of the HbV lipid bilayer membrane. We compared our findings to the corresponding binding rates of a purified human Hb solution suspended in phosphate buffered saline solution (PBS) mixed with pyridoxal 5'-phosphjate (PLP), a solution of polymerized bovine Hb ($poly_BHb$) used for veterinary purposes (Oxyglobin; Biopure Corp. Cambridge, MA) [25], and vesicles containing saline solution.

ACCEPTED MANUSCRIPT

2. Materials and Methods

2.1. Hb-vesicles (HbV), Hb solutions, empty vesicles (EV), and RBCs

HbVs were prepared as reported previously [26-29], with slight modifications. Human Hb solution was obtained through purification of outdated RBCs provided by the Japanese Red Cross Society (Tokyo, Japan). Hb was stabilized by carbonylation (HbCO) and concentrated by ultrafiltration to 38 g/dL. PLP (Sigma, St. Louis, MO) was added to the HbCO solution as an allosteric effector at a molar ratio of PLP/Hb tetramer = 2.5. We use PLP instead of 2,3-diphosphoglyceric acid (2,3-DPG) or inositol hexahosphate (IHP) because 2,3-DPG is very unstable and expensive, and the interaction of IHP and Hb is so strong that the oxygen dissociation curve of Hb is distorted and the Hill number becomes nearly 1 [30].

The Hb solution with PLP was then mixed with lipids and encapsulated in vesicles. The lipid bilayer comprised 1,2-dipalmitoyl-*sn*-glycero-3-phosphatidylcholine (DPPC), cholesterol, 1,5-*O*-dihexadecyl-*N*-succinyl-L-glutamate (Nippon Fine Chemical Co. Ltd., Osaka, Japan), and 1,2-distearoyl-*sn*-glycerol-3-phosphatidylethanolamine-*N*-PEG_{5000} (DSPE-PEG; NOF Corp., Tokyo, Japan) at a molar composition of 5/5/1/0.033. Particle diameter was regulated by extrusion. The encapsulated HbCO was converted to HbO_2 by exposing the liquid membrane of HbV to visible light under an O_2 atmosphere. The particle size distribution was measured using a light-scattering method (Submicron Particle Size Analyzer, model N4 PLUS; Beckman-Coulter, Inc., Fullerton, CA). An empty vesicle (EV) suspension was prepared using the same lipids through hydration with a saline solution. The lipid concentration (6.8 g/dL) and the particle diameter (ca. 250 nm) were almost identical to those of HbV.

A purified human Hb solution suspended in phosphate buffered saline solution (PBS)

was prepared and mixed with PLP at molar ratios of PLP/Hb tetramer = 0 and 2.5. We also used the of polymerized bovine Hb solution (poly$_B$Hb) (Oxyglobin; Biopure Corp. Cambridge, MA) [25]. This solution is a mixture of nonpolymerized tetrameric $_B$Hb (37.2%) and polymerized $_B$Hb with a wide molecular weight distribution [25]. The P_{50} values and Hill numbers of HbV were Hb solutions were obtained from the oxygen equilibrium curve measured using a Hemox-Analyzer (TCS Medical Science, Philadelphia, PA) at 37°C [23,31] **(Figure 1)**.

Blood was harvested from female C57BL/129 mice in accordance with IACUC protocol. RBCs were pelleted at 800g for 30 min and resuspended and washed twice with a 40 mM-HEPES buffer (pH = 7.4, 5 mM glucose, Sigma, St. Louis, MO; tonicity, 285 mOms regulated with NaCl). The RBC suspensions were prepared at concentration of $2x10^6$ cells/mL ([Hb] = 0.93 μM, [heme] = 3.72 μM) in the same HEPES buffer.

2.2. Stopped-flow spectrophotometry

The time course of the ligand binding was analyzed during rapid mixing of the deoxygenated HbV and Hb solutions and a NO- or CO-containing solution using a stopped-flow rapid scan spectrophotometer (RSP-1000; Unisoku Co. Ltd., Osaka, Japan) [22,23]. Solutions in the two gas-tight reservoirs (A and B) are mixed rapidly applying a pressure of 0.3 - 0.6 MPa; the dead time for mixing being < 1.5 ms. All measurements were performed at 25 °C. A PBS solution (3 ml each) was poured into both reservoirs, which were both sealed using septum rubber seals. The reservoirs were deoxygenated by N_2 bubbling for more than 30 min. A stock solution of HbV or Hb (ca. 30 μl, [heme] = 300 μM) was injected into Reservoir A to adjust [heme] to 3 μM and the N_2 bubbling was changed to a flow to avoid denaturation of the solutes. Complete deoxygenation was confirmed using preliminary stopped-flow measurements (wavelength: 385 - 593 nm), where the Soret band showed a

maximum absorbance (λ_{max}) at 430 nm because of the presence of deoxyHb. To make the reservoirs deoxygenated, we did not use sodium dithionate because it is well known that an excess amount of this reagent sometimes possibly induces chemical modifications of heme or globin [32, 33]. In Reservoir B, NO or CO gas bubbling was started while a gentle N_2 flow was maintained in Reservoir A. The mixed gases for NO binding (NO, 0.2029%; N_2, 99.7971%) and for CO binding (CO, 14.14%; N_2, 85.86%) were purchased from Takachiho Chemical Industrial Co., Ltd. (Tokyo).

Stopped flow measurement was initiated after about 10 min bubbling. The sampling interval and the exposure time were set as 1 ms and measurement time was 210 ms. All measurements were performed 3 times and the change of absorbance at 430 nm was plotted as a function of time. The apparent binding rate constants of NO and CO ($k'_{on}{}^{(NO)}$ and $k'_{on}{}^{(CO)}$, respectively) were calculated using Eq. 1 under the assumption of homogeneous distribution of Hb, irreversible second order reaction, and a pseudo-first order reaction when gas molecules are abundant.

$$\ln\frac{\Delta A_t}{\Delta A_0} = -k'_{on}\cdot C_{Gas}\cdot t \qquad (1)$$

In this equation, ΔA_t is the change of absorbance at 430 nm at time t ($= A_t - A_{t=\infty}$) and ΔA_0 is the absorbance at the initial time ($= A_{t=0} - A_{t=\infty}$), and C_{Gas} is the initial gas concentration. NO (1.9 μM) was not much more abundant than the heme concentration (1.5 μM) in the NO-reaction experiments, therefore the apparent binding rates we calculated from the slopes of the initial phase of reactions.

The time courses of the reaction of NO and O_2-bound HbV or HbO_2 solutions were analyzed using stopped-flow spectrometry in the same manner, except that an air-equilibrated

PBS solution was introduced into Reservoir A to ensure the O_2-binding state. The absorption changes were monitored at 408 nm.

2.3. Measurement of NO depletion using a NO electrode

The rate of NO depletion in a test solution after adding NO in an aerobic condition was monitored via an amino-700 probe and an inNO-T sensor (Innovative Instruments, Inc.) connected to a Dell PC running InNO-T software (Innovative Instruments, Inc.) [34]. In a room atmosphere, 3 mL of a PBS solution containing HbV, EV, or mice RBCs was pipetted into a cuvette and stirred using a magnetic stir bar. The NO sensor was introduced into the cuvette for continuous monitoring. After a steady condition was confirmed, a stock NO solution (100 μL) was injected, yielding the concentration of 2 μM NO. The NO level rapidly increases and then decreases with the reaction with O_2 and Hb. Concentrations of the specimens were as follows: HbV ([heme] = 4 μM, [Hb] = 65 mg/L, [Lipid] = 36 mg/L), EV ([lipid] = 36 mg/L), and mice RBC ([heme] = 3.72 μM). Data were fitted and basic statistics and graphs were obtained using Synergy KaleidaGraph 3.6. Correlation was determined using Spearman's rank correlation test, with StatView 5.

ACCEPTED MANUSCRIPT

3. Results

3.1. Stopped-flow spectrophotometry of NO and CO bindings in an anaerobic condition

Complete deoxygenation of HbV was confirmed using the characteristic wavelength of the maximum absorption (λ_{max}) at 430 nm. Because of the stronger light-scattering effect of HbV suspension than that of the Hb solution and RBCs [35], the absorption peaks in the *Q* band region were not well defined in this measurement. After rapid mixing with NO, the immediate absorption reduction at 430 nm and the increase at 418 nm that correspond to the formation of HbNO were confirmed **(Fig. 2a)**. In the case of mixing with CO, the immediate absorption increase at 419 nm was confirmed **(Fig. 2b)**. The change of absorption at 430 nm in both reactions was indicative of the formation of HbNO or HbCO in the vesicles.

The spectrophotometric scans presented in **Figs. 2a and 2b** were performed 3 times and the averaged level of reaction was plotted as a ratio of absorbance at 430 nm (ΔA_t) at time *t*, to the initial absorbance (ΔA_0) at time 0 **(Figs. 3a and 3b)**. Data of Hb solutions are also plotted in those figures. The graph clearly shows that both NO binding and CO binding were slower for HbV than for the human Hb solution without PLP. However, Hb with PLP showed almost identical CO binding to HbV. The NO binding rates of Hb solution with and without PLP and $poly_BHb$ were almost identical. The apparent binding rate constants of $k'_{on}{}^{(NO)}$ for NO and $k'_{on}{}^{(CO)}$ for CO are presented in **Table 1.**

3.2. Stopped-flow spectrophotometry of the reaction of NO and O_2-bound HbV and Hb solutions in an aerobic condition

The oxygenated HbV showed the absorption maximum at 415 nm **(Fig. 2c)**. Mixing with NO showed the immediate reduction of the absorption maximum, although an increase at 405 nm showed attributes of the metHb formation. The spectrophotometry scans portrayed in

Fig. 2c were performed 3 times and the average level of reaction was plotted as a ratio of absorbance at 408 nm ($\Delta A_t = A_t - A_{t=\infty}$) at time t, to the initial absorbance ($\Delta A_0 = A_{t=0} - A_{t=\infty}$) at time 0 **(Fig. 3c)**. The graph shows that the reaction of NO with oxygenated HbV was considerably slower than that of human Hb solutions with and without PLP. The rate of poly$_B$Hb was almost identical to that of human Hb solutions. The apparent oxidation reaction rate constants $k'_{OX}{}^{(NO)}$ are summarized in **Table 1**.

3.3. NO depletion in an aerobic condition in the presence of HbV, RBC, and EV

When the stock NO solution was simply injected into a PBS solution, the NO electrode showed an immediate increase to about 2000 nM, even in the aerobic condition. Then it gradually decreased according to the reaction of NO and O_2 to produce NO_2^- (**Fig. 4**). From the slope after 200 s, the apparent decay constant is calculated as 3.7×10^{-3} s^{-1}. In the case of the presence of EV, the increase in NO concentration immediately after injection and the decay curve were almost identical, and the apparent decay constant was 3.9×10^{-3} s^{-1}. From results of this experiment, it is not clear that the hydrophobic part of the lipid bilayer membrane facilitates NO depletion. The reactions of NO in the aqueous phase are still the prominent ones.

In the presence of HbV, the first injection of NO (2000 nM) was decayed much faster than the sensor was able to record, and only a part of the second NO injection was recorded. The decay curve was finally obtained at the third NO injection when the heme of HbV was totally inactivated with NO and converted to the ferric state. On the other hand, one injection of NO into the RBC suspension clearly showed the decay curve. However, the rate of decay is extremely fast, as indicated by the need for a different time scale of the abscissa. The NO decay constant of HbV was not obtained from this experiment, which has to be analyzed by stopped flow spectrophotometry.

ACCEPTED MANUSCRIPT

4. Discussion

Our primary finding is that NO binding is considerably retarded by encapsulation into phospholipid vesicles, and that CO binding is not influenced by encapsulation, but is slightly retarded by co-encapsulation with PLP as an allosteric effector. In the aerobic condition, the hydrophobic part of the lipid bilayer membrane does not seem to be involved in NO depletion (facilitated reaction with O_2), which is mostly attributable to the reaction with the intracellular Hb solution.

We recently showed that NO binding of Hb is retarded by encapsulation in phospholipid vesicles because of the intracellular diffusion barrier [23]. Intrinsically rapid NO binding causes Hb to become a sink of NO in the interior surface region of HbV, thereby hindering further NO diffusion into the core of HbV, in combination with the lowered diffusion constants of NO in a highly concentrated Hb solution. Using results described in a previous report, we compare two kinds of HbV with different P_{50} values (25 and 14 Torr), and showed that the $k'_{on}{}^{(NO)}$ might change slightly according to P_{50} (0.61×10^7 vs. 0.88×10^7 M^{-1}s^{-1}). Accordingly, the major cause of retardation is Hb encapsulation. Cell-free Hb removes NO much faster (cf. $k'_{on}{}^{(NO)}$ of cell-free Hb solution, 2.4 - 2.6 $\times 10^7$ M^{-1}s^{-1}). Cell-free Hb solutions with and without PLP did not differ greatly. The results coincide well with those in precedent reports: that NO binding to α and β subunits and that the T-state and R-state Hbs are almost identical [36,37]. Poly$_B$Hb that contains high concentration of terameric $_B$Hb and intermolecularly crosslinked tetrameric $_B$Hb are known to induce vasoconstriction and hypertension [38]. In the present study, such Poly$_B$Hb showed identical rapid NO binding.

For CO, we previously reported that CO binding to Hb is intrinsically much slower than NO binding by two orders of magnitude, which allows more time for CO diffusion into the

HbV core. Therefore, $k'_{on}^{(CO)}$ is not influenced by the intracellular Hb concentration and particle size smaller than 500 nm [23]. Results of the present study show the presence of a slight retardation of CO binding by HbV in comparison to the cell-free Hb solution, which is solely attributable to the co-encapsulation of PLP as an allosteric effector. The effector tends to stabilize the T-state and retards CO binding. In contrast to NO, it is well known that cooperative CO binding to four subunits of Hb occurs, and that the binding rate constants to α and β subunits, or T-state and R-state Hbs, are different [39,40]. According to Kwansa et al. [41], the value of $k_{on}^{(CO)}$ of unmodified $_B$Hb measured using stopped flow is 1.3×10^5 $M^{-1}s^{-1}$. Polymerization of $_B$Hb by glutaraldehyde apparently facilitates CO binding ($k_{on}^{(CO)}$ of Poly$_B$Hb = 2.7×10^5 $M^{-1}s^{-1}$).

In the circulation where O_2 is abundant NO is inactivated mainly by NO dioxygenation by O_2-bound HBOCs and RBC. Results of the present study confirmed that the cell-free human Hb solutions with our without PLP showed $k'_{OX}^{(NO)}$ of 7.4 - 8.7 × 10^7 $M^{-1}s^{-1}$, which was faster than that of the reaction of deoxyHb and NO ($k'_{on}^{(NO)}$ = 2.4 - 2.6 × 10^7 $M^{-1}s^{-1}$), a tendency that coincided with the results of Herold et al. [42]. Encapsulation of HbO_2 in vesicles significantly retarded the reaction with NO, and $k'_{OX}^{(NO)}$ was 0.88×10^7 $M^{-1}s^{-1}$. However, we observed the change of heme ligation state (HbO_2 → metHb) and we were unable to observe the NO concentration using stopped-flow spectrophotometry. In an aerobic condition, NO reacts slowly with O_2 to produce NO_2^- in water.

The weight ratio of lipids to Hb of HbVs is about 0.5 - 0.6, this ratio being as low as 0.15 for RBCs. We anticipated that the hydrophobic part of the lipid bilayer membrane of HbV would be involved considerably in NO depletion, as reported by Liu et al. [24], which might affect the results of stopped flow spectrophotometry. We monitored the NO decay in the presence of empty vesicles (without Hb) in an aerobic condition using a NO electrode to

clarify the facilitation of NO depletion. Results show that NO decay in the presence of empty vesicles was almost identical to that in the PBS solution, indicating that the facilitated reaction of NO and O_2 in a hydrophobic part of the lipid bilayer membrane is negligibly small compared to the reaction with the intracellular Hb.

This finding may be related to the lipid composition of the membrane. The saturated phospholipid (DPPC, phase transition temperature = 41 °C) with cholesterol in HbV might be more resistant to oxidative damage than is soy phosphatidylcholine reported by Liu et al. [24], which probably contains many unsaturated fatty acids. Moreover, nitration of unsaturated bonds might occur, which is another pathway for NO depletion [43]. Conversely, our lipid mixture of DPPC comprises saturated fatty acids and cholesterol providing a hydrophobic rigid domain that would differ from the liposomes made of soy phospholipids. If the aqueous reaction of NO and dioxygen occurs with overall stoichiometry of $4NO + O_2 + 2H_2O \rightarrow 4H^+ + 4NO_2^-$ [24,44], then H_2O is required even in the hydrophobic part. The unstable soy phospholipid vesicles in the literatures would provide more water molecules than does the rigid and stable bilayer membrane of our HbV. Accordingly, we conclude that NO depletion in aerobic conditions in the presence of HbV is caused primarily by the encapsulated Hbs, and the contribution of the bilayer membrane of HbV is negligibly small.

The NO decay in HbV was much faster than that for RBCs. In addition, measurements using the NO electrode were unable to detect the reaction rate of O_2-HbV and NO. These results demonstrate that NO mainly reacts with Hb in HbV. Given the rate of NO decay shown in Figure 4, we can assume that less than 0.1% of total NO (1.9 μM) reacts with the physically-dissolved O_2 in PBS in 200 ms after the rapid mixing by stopped flow spectrophotometry.

In a previous report on the relative magnitude of the binding rate constant of NO (fast) and CO (slow) to deoxygenated HbV, we predicted that the strength of the diffusion barrier induced in HbV becomes more significant with the faster ligand binding reaction with Hb [23]. According to our results and Herold et al. [42], the elementary reaction of NO and HbO_2 is much faster than that of NO with deoxyHb. As shown in Figure 2, Hb encapsulation in vesicles retarded NO binding to deoxyHb by 1/4, and NO reaction with HbO_2 by 1/8. The impact of Hb encapsulation on the reaction with NO is strengthened in the aerobic condition.

We previously reported that HbV does not induce hypertension. However, present results, which show retardations of NO binding by encapsulation and CO binding by co-encapsulation of PLP in comparison to cell-free Hb solutions and poly$_B$Hb, cannot fully explain the absence of vasoconstriction or hypertension after intravenous injection because these reactions of HbV are much greater than those of RBCs (10^4 - 10^5 $M^{-1}s^{-1}$) [1,2,37,45]. Any Hb-based oxygen carrier (HBOC) is much smaller than an RBC and is distributed homogeneously in the plasma layer [46]. Consequently, an RBC-free zone at the blood/endothelium interface becomes an HBOC-containing zone, and might be a sink of NO [47,48]. Rohlfs et al. [49] reported that NO binding rate constants of a series of chemically modified HBOCs (diameter, 6 - 28 nm), measured using the laser flash photolysis, were identical to that of an unmodified Hb solution: 3.0×10^7 $M^{-1}s^{-1}$. They concluded straightforwardly that NO uptake was unrelated to vasoconstriction because PEG-modified Hb did not induce vasoconstriction, other mechanisms being suggested as determinants of vasoconstriction such as molecular recognition, oxygen affinity [7,50] and facilitated diffusion. Poly$_B$Hb is larger than monomeric $_B$Hb, but may be vasoactive because of the presence of monomeric $_B$Hb and its high P_{50} [25,31].

It is also speculated that there is a threshold particle diameter to penetrate across the

perforated endothelial cell layer to approach a space (such as the space of Disse near the sinusoidal endothelial layer in a hepatic microcirculation, or the space between the endothelium and the smooth muscle), where CO or NO is produced as a vasorelaxation factor. Because the particle size of HbV (250 nm) is obviously much larger than Hb tetramer and its polymerized form as shown in **Figure 5**. Both the retardation of NO reaction and the larger particle diameter are inferred to be keys to suppress vasoconstriction and hypertension induced by HBOCs.

In conclusion, the source of vasoactivity of HBOCs has been extensively reviewed [7,9,13,38,51-54] and it is generally agreed that NO scavenging is a factor in this process, although it does not provide an all encompassing explanation. In terms of HbV, the intrinsically fast reactions of NO with the cell-free Hb solutions in both aerobic and anaerobic conditions are considerably retarded by the encapsulation process. Therefore, since NO bioavailability results from the balance of the rate of NO production and NO entrapment or scavenging, the finding that the latter processes are significantly retarded in HbVs provides some meaningful information to explain their vasoinactivity.

Acknowledgments

The authors would like to thank Dr. Hirohisa Horinouchi (Keio University), Dr. Amy G. Tsai and Dr. Pedro Cabrales (University of California, San Diego), and Dr. Keitaro Sou (Waseda University) for valuable discussions. This work was supported in part as Health Sciences Research including Drug Innovation from the Ministry of Health, Labour and Welfare, Japan, Grants in Aid for Scientific Research (B) from the Japan Society for the Promotion of Science (19300164), and USPHS Bioengineering Research Partnership grant R24-HL 64395, R01-HL62354 and P01-HL71064.

REFERENCES

[1] E. Carlsen, J.H. Comroe, The rate of uptake of carbon monoxide and of nitric oxide by normal human erythrocytes and experimentally produced spherocytes, J. Gen. Physiol. 42 (1958) 83-107

[2] X. Liu, M.J. Miller, M.S. Joshi, H. Sadowska-Krowicka, D.A. Clark, J.R. Jr. Lancaster, Diffusion-limited reaction of free nitric oxide with erythrocytes, J. Biol. Chem. 273 (1998) 18709-19713

[3] M.W. Vaughn, K.T. Huang, L. Kuo, J.C. Liao, Erythrocytes possess an intrinsic barrier to nitric oxide consumption, J. Biol. Chem. 275 (2000) 2342-2348.

[4] P.C. Minneci, K.J. Deans, H. Zhi, P.S. Yuen, R.A. Star, S.M. Banks, A.N. Schechter, C. Natanson, M.T. Gladwin, S.B. Solomon, Hemolysis-associated endothelial dysfunction mediated by accelerated NO inactivation by decompartmentalized oxyhemoglobin, J. Clin. Invest. 115 (2005) 3409-3417.

[5] J.R. Hess, V.W. MacDonald, W.W. Brinkley, Systemic and pulmonary hypertension after resuscitation with cell-free hemoglobin, J. Appl. Physiol. 74 (1993) 1769-1778.

[6] E.P. Sloan, M. Koenigsberg, D. Gens, M. Cipolle, J. Runge, M.N. Mallory, G. Jr. Rodman, Diaspirin cross-linked hemoglobin (DCLHb) in the treatment of severe traumatic hemorrhagic shock: a randomized controlled efficacy trial, JAMA 282 (1999) 1857-1864.

[7] A. Gulati, A. Barve, A.P. Sen, Pharmacology of hemoglobin therapeutics, J. Lab. Clin. Med. 133 (1999) 112-119.

[8] G. Rochon, A. Caron, M. Toussaint-Hacquard, A.I. Alayash, M. Gentils, P. Labrude, J.F. Stoltz, P. Menu, Hemodilution with stroma-free hemoglobin at physiologically maintained viscosity delays the onset of vasoconstriction, Hypertension 43 (2004) 1110-1115.

ACCEPTED MANUSCRIPT

[9] H. Sakai, H. Hara, M. Yuasa, A.G. Tsai, S. Takeoka, E. Tsuchida, M. Intaglietta, Molecular dimensions of Hb-based O_2 carriers determine constriction of resistance arteries and hypertension, Am. J. Physiol. Heart Circ. Physiol. 279 (2000) H908-H915.

[10] K. Nakai, T. Ohta, I. Sakuma, K. Akama, Y. Kobayashi, S. Tokuyama, A. Kitabatake, Y. Nakazato, T.A. Takahashi, S. Sekiguchi, Inhibition of endothelium-dependent relaxation by hemoglobin in rabbit aortic strips: comparison between acellular hemoglobin derivatives and cellular hemoglobins, J. Cardiovasc. Pharmacol. 28 (1996) 115-123.

[11] J.S. Olson, E.W. Foley, C. Rogge, A.L. Tsai, M.P. Doyle, D.D. Lemon, No scavenging and the hypertensive effect of hemoglobin-based blood substitutes, Free Radic. Biol. Med. 36 (2004) 685-697.

[12] M. Suematsu, N. Goda, T. Sano, S. Kashiwagi, T. Egawa, Y. Shinoda, Y. Ishimura, Y. Carbon monoxide: an endogenous modulator of sinusoidal tone in the perfused rat liver. J. Clin. Invest. 96 (1995) 2431-2437.

[13] N. Goda, K. Suzuki, M. Naito, S. Takeoka, E. Tsuchida, Y. Ishimura, T. Tamatani, M. Suematsu, Distribution of heme oxygenase isoforms in rat liver. Topographic basis for carbon monoxide-mediated microvascular relaxation, J. Clin. Invest. 101 (1998) 604-612.

[14] X. Liu, A. Samouilov, J.R. Jr. Lancaster, J.L. Zweier, Nitric oxide uptake by erythrocytes is primarily limited by extracellular diffusion not membrane resistance, J. Biol. Chem. 277 (2002) 26194-26199.

[15] D.B. Kim-Shapiro, A.N. Schechter, M.T. Gladwin, Unraveling the reactions of nitric oxide, nitrite, and hemoglobin in physiology and therapeutics, Arterioscler. Thromb. Vasc. Biol. 26 (2006) 697-705.

[16] K.T. Huang, Z. Huang, D.B. Kim-Shapiro, Nitric oxide red blood cell membrane permeability at high and low oxygen tension, Nitric Oxide 16 (2007) 209-216.

[17] K.T. Huang, T.H. Han, D.R. Hyduke, M.W. Vaughn, H. Van Herle, T.W. Hein, C.